ARTICLE IN PRESS

主論文

ELSEVIER

PEPTIDES
AN INTERNATIONAL JOURNAL

Available online at
ScienceDirect

Brain-specific natriuretic peptide receptor-B deletion attenuates high-fat diet-induced visceral and hepatic lipid deposition in mice

Yui Yamashita[a], Nobuko Yamada-Goto[b,*], Goro Katsuura[a], Yukari Ochi[a], Yugo Kanai[a], Yuri Miyazaki[c], Koichiro Kuwahara[d], Naotetsu Kanamoto[a], Masako Miura[a], Akihiro Yasoda[a], Kousaku Ohinata[c], Nobuya Inagaki[a], Kazuwa Nakao[e]

[a] Department of Diabetes, Endocrinology and Nutrition, Kyoto University Graduate School of Medicine, 54, Shogoin Kawahara-cho, Sakyo-ku, Kyoto 606-8507, Japan
[b] Division of Endocrinology, Metabolism and Nephrology, Department of Internal Medicine, Keio University, School of Medicine, 35, Shinano-machi, Shinjyuku-ku, Tokyo 160-8582, Japan
[c] Division of Food Science and Biotechnology, Kyoto University Graduate School of Agriculture, Gokasyo, Uji-shi, Kyoto 611-0011, Japan
[d] Department of Cardiovascular Medicine, Kyoto University Graduate School of Medicine, 54 Shogoin Kawahara-cho, Sakyo-ku, Kyoto 606-8507, Japan
[e] Kyoto University Graduate School of Medicine Medical Innovation Center, 53, Shogoin Kawahara-cho, Sakyo-ku, Kyoto 606-8507, Japan

ARTICLE INFO

ABSTRACT

C-type natriuretic peptide (CNP) and its receptor, natriuretic peptide receptor-B (NPR-B), are abundantly distributed in the hypothalamus. To explore the role of central CNP/NPR-B signaling in energy regulation, we generated mice with brain-specific NPR-B deletion (BND mice) by crossing Nestin-Cre transgenic mice and mice with a *loxP*-flanked NPR-B locus. Brain-specific NPR-B deletion prevented body weight gain induced by a high-fat diet (HFD), and the mesenteric fat and liver weights were significantly decreased in BND mice fed an HFD. The decreased liver weight in BND mice was attributed to decreased lipid accumulation in the liver, which was confirmed by histologic findings and lipid content. Gene expression analysis revealed a significant decrease in the mRNA expression levels of CD36, Fsp27, and Mogat1 in the liver of BND mice, and uncoupling protein 2 mRNA expression was significantly lower in the mesenteric fat of BND mice fed an HFD than in that of control mice. This difference was not observed in the epididymal or subcutaneous fat. Although previous studies reported that CNP/NPR-B signaling inhibits SNS activity in rodents, SNS is unlikely to be the underlying mechanism of the metabolic phenotype observed in BND mice.

Taken together, CNP/NPR-B signaling in the brain could be a central factor that regulates visceral lipid accumulation and hepatic steatosis under HFD conditions. Further analyses of the precise mechanisms will enhance our understanding of the contribution of the CNP/NPR-B system to energy regulation.

1. Introduction

C-type natriuretic peptide (CNP) exerts its biologic effects by binding to natriuretic peptide receptor-B (NPR-B), a membrane-bound guanylyl cyclase receptor that produces cyclic guanylyl monophosphate (cGMP) [1]. CNP is expressed in a wide variety of tissues, such as brain, vascular endothelium, heart, bone, and adrenal and reproductive glands [2–6]. NPR-B is also widely expressed in a large variety of tissues, such as lung, brain, adrenal gland, kidney, uterus, ovary, heart, vascular smooth muscle, and chondrocytes [7]. Among these tissues, CNP and NPR-B mRNA are both highly expressed in the brain, particularly in discrete hypothalamic areas, such as the arcuate nucleus of the hypothalamus, which is an important center for energy regulation [8–11]. These findings suggest that the brain CNP/NPR-B system is involved in the regulation of energy homeostasis. The physiologic significance of CNP/NPR-B signaling in energy regulation, however, has not been elucidated well because disruption of either the CNP or NPR-B gene results in dwarfism and early death due to impaired endochondral ossification [12,13].

We previously generated CNP-null mice with chondrocyte-targeted CNP expression (CNP-Tg/Nppc-/- mice), in which marked skeletal dysplasia was rescued, and investigated the role of CNP in body weight control and metabolic homeostasis. Based on previous observations of CNP-Tg/Nppc-/- mice, CNP/NPR-B signaling centrally inhibits sympathetic nervous system (SNS) activity and thermogenesis in brown adipose tissue [14]. More recently, we reported that intracerebroventricular administration of CNP significantly suppresses fasting-induced refeeding and nocturnal food intake in mice [15].

In the present study, to further investigate the physiologic significance of a brain CNP/NPR-B signaling in energy regulation, we generated mice with brain-specific NPR-B deletion (BND mice) using the Cre/loxP system and investigated the role of the central CNP/NPR-B system in body weight control and metabolic homeostasis.

2. Materials and methods

2.1. Animals

Mice were maintained under 14:10 h light:dark cycles (lights on at 0700 h; lights off at 2100 h) at 23 °C. Food and water were available ad libitum unless otherwise stated. All animal experiments were performed in accordance with the ethical guidelines of Kyoto University and the United States National Institutes of Health Guide for the Care and Use of Laboratory Animals. Every effort was made to optimize comfort and to minimize the use of animals. This project was approved by the Animal Research Committee, Graduate School of Medicine, Kyoto University.

2.2. Generation of BND mice

Nestin-Cre mice, which express the Cre recombinase specifically in neuronal and glial precursor cells, were generated in a C57BL/6 background, as described previously [16]. Briefly, for construction of the Nestin-Cre transgene, the 2.5-kb NotI-SalI fragment of the nestin promoter, the Cre recombinase fragment, and the 5.3-kb BamHI fragment of the three nestin introns, which contains a neural precursor-specific enhancer, were ligated into a pBluescript vector in that order (S1 Fig.) [16]. We generated a modified NPR-B allele in embryonic stem (ES) cells by inserting a loxP site together with a neo marker flanked by two-flippase recognition targets (frt). A targeting vector for ES cells that contained a fragment of the NPR-B gene was designed to generate conditional knockout mice in which the region from exon 3 to exon 7 of the NPR-B gene was removed using the Cre/loxP gene targeting strategy. Briefly, a genomic clone containing the NPR-B gene was obtained from a C57BL/6 mouse BAC clone. The region from exon 3 to exon 7 of the NPR-B gene was subcloned into a pBluescript II SK (+) vector and a loxP was inserted upstream of NPR-B exon 3 (loxP-Exon). The 2.7-Kb NotI-SacII fragment was subcloned into a pBluescript vector downstream of a frt-neo-frt-loxP cassette (frt-neo-frt-loxP-short). The 5.2-Kb XhoI-ClaI fragment was also subcloned into a pBluescript vector downstream of the diphtheria toxin A fragment gene (DTA-long). At this point, the loxP-Exon fragment was subcloned into the pBluescript vector carrying the DTA-long fragment (DTA-long-loxP-Exon). To generate the targeting vector, the frt-neo-frt-loxP-short fragment was subcloned into the pBluescript vector carrying the DTA-long-loxP-Exon fragment. Correct assembly of this vector was confirmed by DNA sequencing.

C57BL/6 ES cells were transfected with the targeting vector by electroporation. Germline chimeric mice were generated by injecting C57BL/6 ES cells into BALB/c blastocysts. Chimeric mice with a high ES cell contribution were crossed with C57BL/6 mice to gener-

ate NPR-B$^{loxP-neo/+}$ mice. The Neo gene was subsequently removed by flp-mediated recombination in vivo, by crossing NPR-B$^{loxP-neo/+}$ offspring with flp-expressing deleter mice. The genotypes of the mice were determined by PCR analyses using genomic DNA isolated from tail tips.

2.3. Diet-induced obesity

Male mice were fed a standard diet (SD; F-2; 12% calories from fat, Funabashi Farms, Japan) at weaning and switched to a high-fat diet (HFD; D12492; 60% calories from fat, Research Diets, New Brunswick, NJ) at 8 week of age. Body weight was measured once a week. For food intake measurements, the mice were housed individually and food weight was measured once a week. Cumulative food intake data were obtained by adding all intake measurements during the study. Mice were killed by cervical dislocation after 8 weeks on the HFD, and the hypothalamus, liver, heart, white adipose tissues (epididymal, mesenteric, and subcutaneous adipose tissues), brown adipose tissue, and soleus were collected. To examine the effects of short-term exposure to HFD, 8-week-old mice were fed either the SD or HFD for a week. At 9 weeks of age, the animals were killed for further analyses.

2.4. Oxygen consumption, locomotor activity, and core body temperature

Male mice at 16–20 weeks of age were individually placed in air-tight 15 × 15 × 15 cm plastic cages, and oxygen consumption were measured for 3 days by indirect calorimetry with a model MK-5000RQ using the analysis software MMS-2 (Muromachi Kikai, Tokyo, Japan). Spontaneous locomotor activity was measured in a SUPERMEX apparatus with analysis software CompACT AMS (Muromachi Kikai, Tokyo, Japan). Mice were acclimated to the monitoring for 1 h once a day for 3 days before the 72-h recording. Rectal temperature was measured as core body temperature with a digital thermometer at 1000, 1600, and 2200 h. A sensor was inserted 1 cm from the anus.

2.5. Metabolic analysis

For plasma metabolic parameter measurements, blood was collected from freely fed mice at 16 weeks of age. Plasma triglyceride, total cholesterol, free fatty acid, and glucose concentrations were measured using commercial assay kits according to the manufacturer's directions (Triglyceride E-test, Cholesterol E-test, NEFA C-test, Glucose CII-test, Wako Pure Chemical, Osaka, Japan). Plasma insulin, leptin, growth hormone, and IGF-I levels were measured by ELISA using a commercial assay kit (mouse insulin ELISA kit, Sibayagi, Gunma, Japan; mouse leptin ELISA, Millipore, Billerica, MA, USA; Rat/Mouse Growth Hormone ELISA, Millipore; and Mouse/Rat IGF-I Quantikine ELISA Kit, R&D Systems, MN, USA) according to the manufacturer's directions.

2.6. Measurement of the lipid content in tissues (liver, white adipose tissue, and soleus) and feces

Tissues (liver, white adipose tissue, and soleus) were isolated from mice and immediately frozen in liquid nitrogen and feces were collected for 1 week. Lipids in tissues and feces were extracted with isopropyl alcohol/heptane (1:1 vol/vol). After evaporating the solvent, the lipids were resuspended in 99.5% (vol/vol) ethanol, and the triglyceride and cholesterol contents were measured using a Triglyceride E-test Wako kit and Cholesterol E-test Wako kit, respectively.
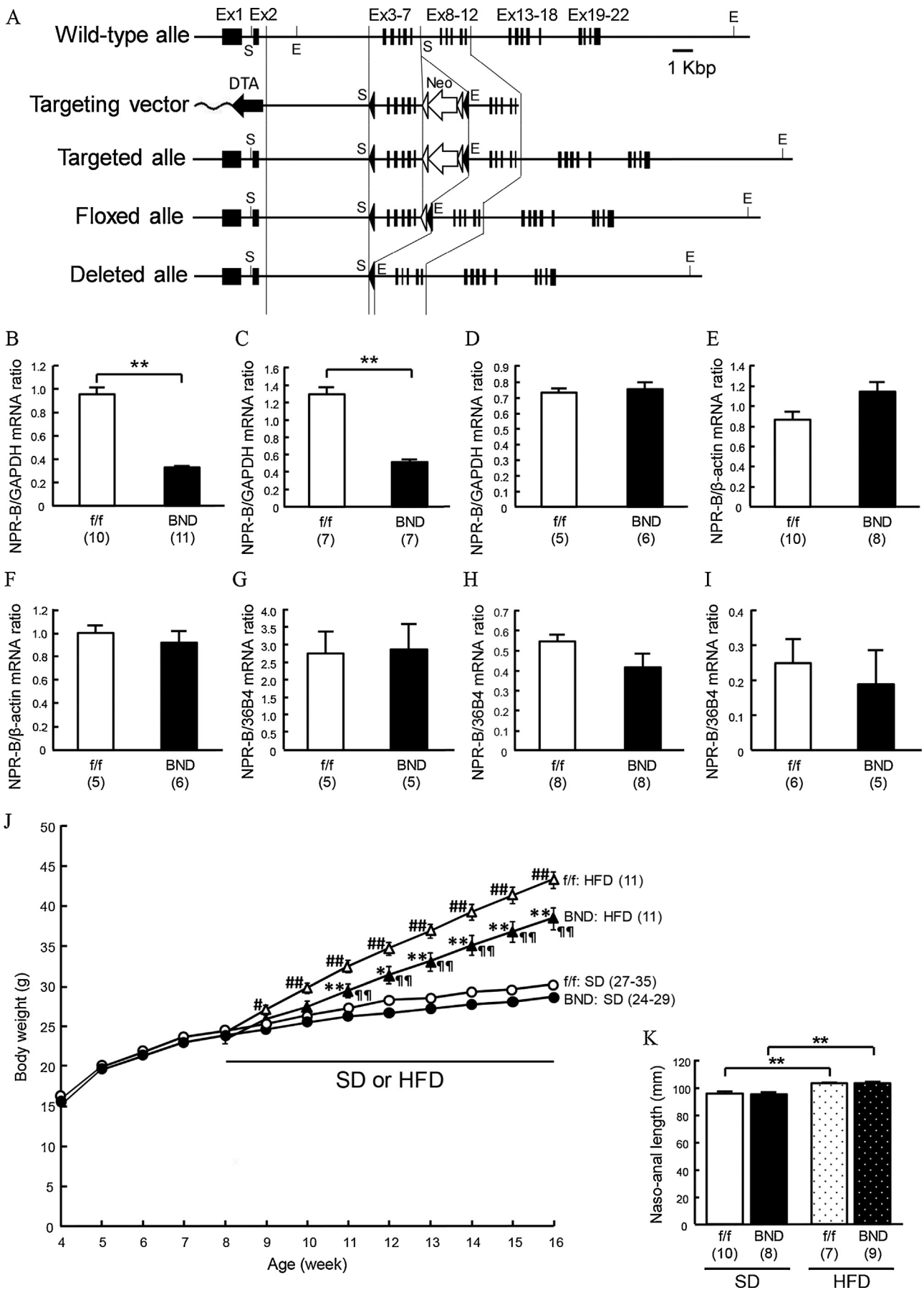
Fig. 1. Generation of BND mice. (A) Structure of the targeting construct of the floxed mice. Scheme of the wild-type gene locus, targeting vector, and resulting alleles (closed triangles, *loxP*; open triangles, *frt*; S, SacI; E, EcoRI). (B) NPR-B mRNA expression levels in the hypothalamus, (C) cerebellum, (D) heart, (E) liver, (F) brown adipose tissue, (G)

2.7. Measurement of tissue norepinephrine content

Tissues (liver and white adipose) were isolated from mice at 16 weeks of age and immediately frozen in liquid nitrogen. Tissue samples were homogenized in 1 mL of ice-cold 0.4 N $HClO_4$ buffer (containing 2 g/L EDTA-2Na and 20 mg/L ascorbic acid) and centrifuged at 3500 rpm for 20 min at 4 °C. Norepinephrine was determined by HPLC in SRL, Tokyo, Japan.

2.8. Liver histology

For histologic analysis, livers were fixed in 10% neutral buffered formalin for 48 h, then immersed in 30% sucrose, embedded in O.C.T. compound (Sakura Finetek Japan, Tokyo, Japan), and stored at −80 °C until sectioning. O.C.T.-embedded tissues were cut into 20-μm sections on a cryostat, and mounted on slides. Tissue sections were subsequently stained with hematoxylin and eosin or 0.6% Oil Red O solution (60% isopropanol, 40% water).

2.9. RNA extraction, cDNA synthesis, and real-time PCR

Total cellular RNA was extracted using the RNeasy Mini Kit (Qiagen, Hilden, Germany) according to the manufacturer's protocol. Then, cDNA was synthesized from total RNA using SuperScript III reverse transcriptase (Invitrogen Corp., Carlsbad, CA, USA), according to the manufacturer's protocol. Gene expression was assessed by quantitative real-time PCR using SYBR Green dye on an Applied Biosystems 7300 Real-time PCR system (Applied Biosystems, Foster City, CA, USA) with the appropriate primers (S1 Table).

2.10. Protein extraction and western blot analysis

Tissue extracts were prepared by homogenization in a lysis buffer (25 mM Tris-HCl, pH 7.4, 50 mM sodium pyrophosphate, 100 mM sodium fluoride, 10 mM EDTA, 1% NP-40, 1 mM phenylmethylsulfonyl fluoride, 1 mM sodium orthovanadate, 10 μg/ml aprotinin, and 10 μg/ml leupeptin). After separation of each lysate (30 μg) by SDS-PAGE, the proteins were transferred to a polyvinylidene difluoride membrane, which was blotted overnight with primary antibody at 4 °C. After blotting with the appropriate secondary horseradish peroxidase-labeled antibodies for 1 h at room temperature, signals were detected using ECL Prime Western Blotting Detection Reagent (GE Healthcare Bio-sciences Corp., Piscataway, NJ, USA) by chemiluminescence.

In this study, the following antibodies were used: rabbit polyclonal antibody directed to uncoupling protein 1 (UCP1) (1:1000; ab10983; Abcam, Cambridge, UK) and mouse monoclonal antibody directed to glyceraldehyde-3-phosphate dehydrogenase (GAPDH) (1:1000; sc-32233; Santa Cruz Biotechnology, Inc., Dallas, TX, USA). Image acquisition was analyzed using ImageQuant TL software.

2.11. Statistical analysis

All values are expressed as the mean ± SEM. Statistical analysis of the data was performed by ANOVA followed by the Tukey-Kramer test. Statistical significance was defined as $P < 0.05$.

3. Results

3.1. Generation of BND mice

The structures of the targeting construct used to generate floxed mice are shown in Fig. 1A. In NPR-B^{flox} mice, a targeting vector was constructed so that exons 3–7, which encode the C-terminal half of the extracellular ligand-binding domain and the transmembrane segment, were flanked by the loxP sites. Nestin-Cre mice were crossed with NPR-B$^{flox/flox}$ mice to generate Cre$^{+/−}$NPR-B$^{flox/flox}$ (BND mice) and Cre$^{−/−}$NPR-B$^{flox/flox}$ (floxed; f/f) mice. Theoretically, BND mice do not express any isoforms of the NPR-B protein in the central nervous system (CNS). Nestin-Cre mice must be used with caution in metabolic studies as there is a reported metabolic phenotype [17]. We examined the body weight of Nestin-Cre mice at the beginning of the study. Growth curves indicated no differences in body weight between wild-type mice, Nestin-Cre mice, and floxed (f/f) mice (S2 Fig. A and B). Therefore, we used floxed mice as controls in the experiments reported below. The Cre-mediated deletion of NPR-B was confirmed by reversetranscription-PCR. NPR-B mRNA expression in the hypothalamus and cerebellum in BND mice was reduced to one-third that of controls (Fig. 1B and C), whereas expression in the heart, liver, brown adipose tissue, and white adipose tissue remained unchanged (Fig. 1D–I), indicating brain-specific NPR-B deletion.

3.2. Changes in body weight and body length in BND mice

To investigate whether brain-specific NPR-B deletion affects systemic energy regulation, we first determined the body weight of the mice. Body weights of BND and control mice fed an SD were indistinguishable. When fed an HFD, however, BND mice had significantly lower body weight gain than control mice (Fig. 1J). At 16 week of age, the body weight of BND mice fed an HFD was 11% lower than that of control mice. Although previous studies reported that systemic CNP or NPR-B knockout mice had a shorter stature due to impaired bone growth [12,13], the naso-anal length was comparable between BND mice and control mice fed either an SD or HFD (Fig. 1K).

3.3. Parameters for energy balance

To investigate the mechanism underlying decreased body weight in BND mice fed an HFD, we measured cumulative food intake over an 8-week period and assessed energy expenditure. Food intake did not differ significantly between BND and control mice fed either an SD or HFD (Fig. 2A). In addition, there was no difference in the oxygen consumption, respiratory quotient, or locomotor activity between BND and control mice fed either an SD or HFD (Fig. 2B and S3 Fig. A and B). Further, there was no difference in core body temperature between BND and control mice fed either an SD or HFD (Fig. 2C). Consistent with these results, the expression levels of UCP1 mRNA and protein in the brown adipose tissue did not differ significantly between BND and control mice fed either an SD or HFD (Fig. 2D and E). To exclude the possibility that food malabsorption contributed to the reduced body weight of BND mice fed an HFD, we also measured the fecal triglyceride content, and found no difference between BND and control mice fed an HFD (Fig. 2F).

mesenteric fat, (H) epididymal fat, and (I) subcutaneous fat (real-time quantitative PCR). Data were normalized to GAPDH, β-actin, or 36B4 mRNA. *$P < 0.05$, **$P < 0.01$. (J) Body weight changes of control mice on an SD (f/f: SD, open circles), BND mice on an SD (BND: SD, closed circles), control mice on an HFD (f/f: HFD, open triangles), and BND mice on an HFD (BND: HFD, closed triangles). Mice were weighed weekly from 4 weeks of age. At 8 weeks of age, mice were given either an SD or HFD. *$P < 0.05$, **$P < 0.01$ vs. f/f: HFD group. #$P < 0.05$, #$P < 0.01$ vs. f/f: SD group. ¶$P < 0.05$, ¶¶$P < 0.01$ vs. BND: SD group. (K) Body length (naso-anal length) at 16 weeks of age fed an SD or HFD. Values are means ± SEM. Number of animals is indicated in parentheses.
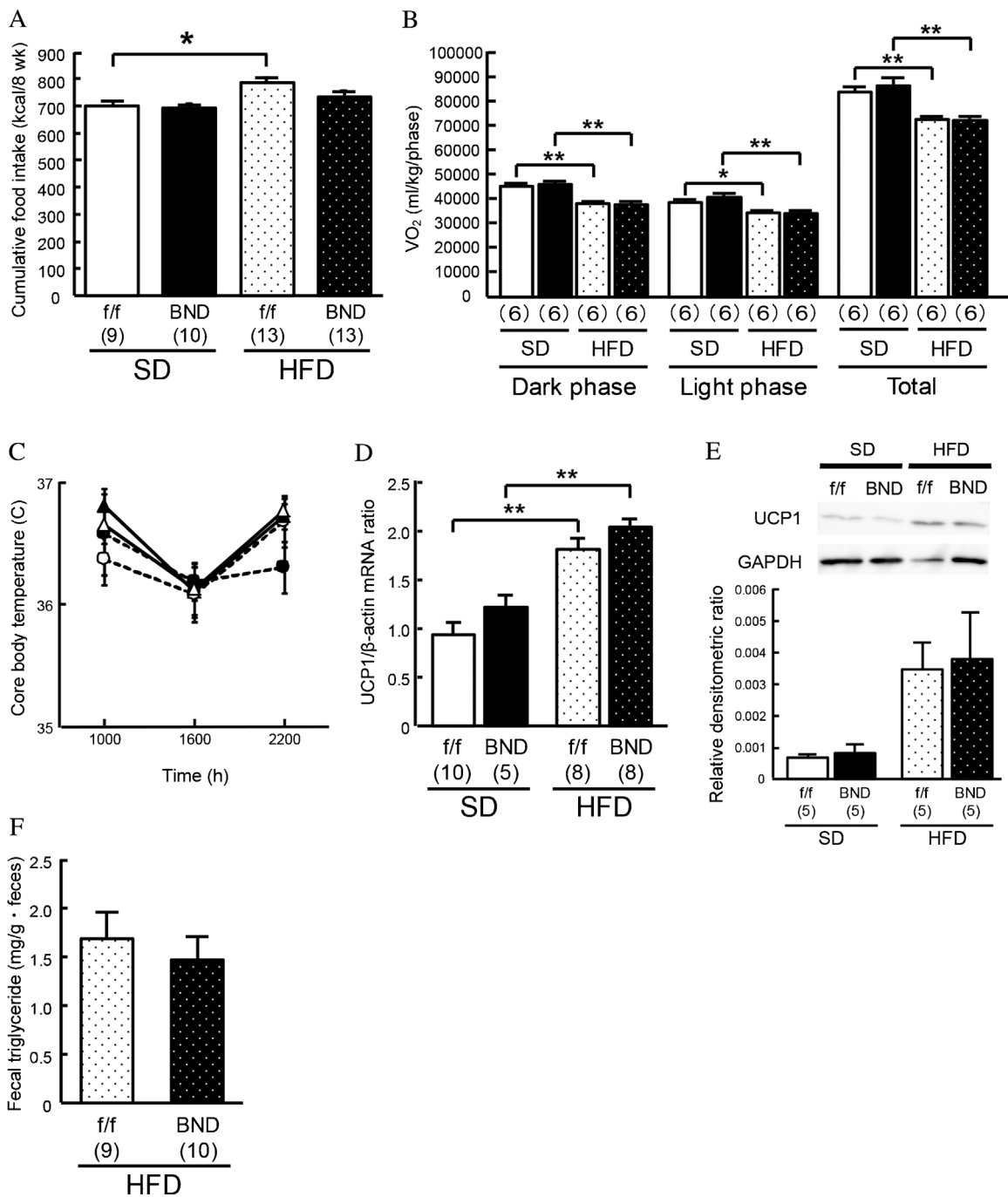
Fig. 2. Energy balance parameters. (A) Cumulative food intake of mice fed an SD or HFD for 8 weeks (from 8 to 16 weeks of age). (B) Oxygen consumption in control mice fed an SD (white bar), BND mice fed an SD (black bar), control mice fed an HFD (white bar with black dots), and BND mice fed an HFD (black bar with white dots). Mice (16–20 weeks old) were acclimated individually in metabolic cages, and experiments were performed for 3 days on an SD or HFD. Data were normalized by body weight and were the sum of light or dark phases from 3-day measurements. (C) Changes in core body temperature of control mice on an SD (open circles with dashed line, n = 9), BND mice on an SD (closed circles with dashed line, n = 11), control mice on an HFD (open triangles with solid line, n = 9), and BND mice on an HFD (closed triangles with solid line, n = 7). (D) UCP1 mRNA expression levels in the brown adipose tissue. Data were normalized to β-actin mRNA. (E) UCP1 protein expression in the brown adipose tissue. Western blot image (upper panel) and densitometric analysis (lower panel) of UCP1 protein expression. (F) Triglyceride contents in the feces of mice fed an HFD. *$P < 0.05$, **$P < 0.01$. Values are means ± SEM. Number of animals is indicated in parentheses.

3.4. Changes in plasma metabolic parameters in BND mice

We then evaluated the effect of brain-specific NPR-B deletion on plasma metabolic parameters. Plasma glucose concentrations were similar between BND mice and control mice fed either an SD or HFD (Fig. 3A). Plasma insulin levels were significantly increased with HFD feeding in both BND and control mice. BND mice fed an HFD exhibited significantly reduced plasma insulin concentrations in the fed state (Fig. 3B). In addition, under HFD feeding, plasma cholesterol levels were significantly decreased in BND mice compared with control mice (Fig. 3C). There were no significant differences in the triglyceride and free fatty acid concentrations between BND and control mice (Fig. 3D and E). Consistent with changes in body weight, plasma leptin levels were significantly
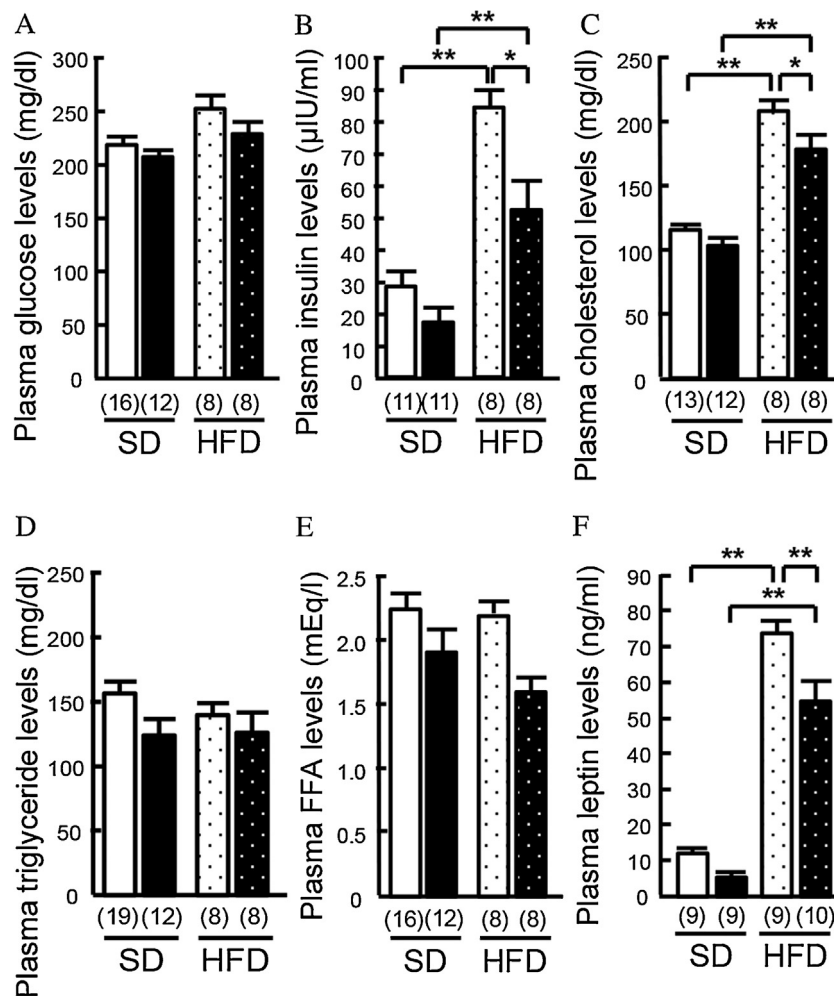
Fig. 3. Changes in plasma metabolic parameters in BND mice. Plasma concentrations of glucose, insulin, triglyceride, cholesterol, and free fatty acid (FFA) in control and BND mice fed ad libitum. (A) Glucose, (B) insulin, (C) cholesterol, (D) triglyceride, (E) FFA, and (F) leptin were determined in mice at 16 weeks of age fed an SD or HFD. White bar = control mice fed an SD; black bar = BND mice fed an SD; white bar with black dots = control mice fed an HFD; black bar with white dots = BND mice fed an HFD. $*P < 0.05$, $**P < 0.01$. Values are means ± SEM. Number of animals is indicated in parentheses.

increased with HFD feeding in both BND and control mice. When fed an HFD, BND mice had significantly lower leptin levels than control mice (Fig. 3F).

3.5. Changes in tissue weight in BND mice

We measured the weights of the liver, heart, mesenteric fat, and epididymal fat after 8 weeks of HFD feeding. Liver weight was decreased by 27% in BND mice fed an HFD compared with control mice (Fig. 4A). Moreover, the mesenteric fat weight was decreased by 37% in BND mice fed an HFD compared with control mice (Fig. 4B). In contrast, the weight of the epididymal fat and heart did not differ between BND mice and control mice fed either an SD or HFD (Fig. 4C and D).

3.6. Effects of brain-specific NPR-B deletion on the liver

An HFD leads to the accumulation of lipids in the liver and eventually hepatic steatosis. The liver of control mice fed an HFD for 8 weeks appeared yellowish, suggesting hepatic steatosis (Fig. 5A). In contrast, the liver of BND mice fed an HFD appeared reddish and was similar to that of control mice fed an SD (Fig. 5A). The liver in the SD-fed group appeared almost normal upon histologic examination. In HFD-fed mice of both genotypes, however, there were fat globules in the hepatocyte cytoplasm and the cell lining

of the hepatic cords appeared abnormal (Fig. 5B). These changes were more obvious in control mice. Oil red O staining further confirmed that HFD-induced fatty changes in the liver were reduced in BND mice. Lipid droplets were sparser in liver sections from BND mice compared with control mice (Fig. 5B). Consistent with these observations, the liver triglyceride and cholesterol content was significantly lower in BND mice than in control mice fed an HFD (Fig. 5C and D). To identify the molecular mechanisms responsible for the decreased liver weight and hepatic lipid accumulation in BND mice fed an HFD, we analyzed the mRNA expression of genes involved in lipid metabolism. Expression levels of none of the several genes tested differed significantly between BND and control mice fed an HFD, but the expression of CD36, which facilitates the cellular uptake of fatty acid; fat-specific protein 27 (Fsp27), which plays a critical role in triglyceride accumulation; and monoacylglycerol *O*-acyltransferase one (Mogat1), which is part of an alternative pathway of triglyceride synthesis, were significantly lower in BND mice fed an HFD than in control mice (Fig. 5E–P).

3.7. Effects of brain-specific NPR-B deletion on white adipose tissue and skeletal muscle

Whereas the epididymal fat weight did not differ between BND and control mice, the mesenteric fat weight was decreased in BND mice fed an HFD compared with control mice (Fig. 4C). To
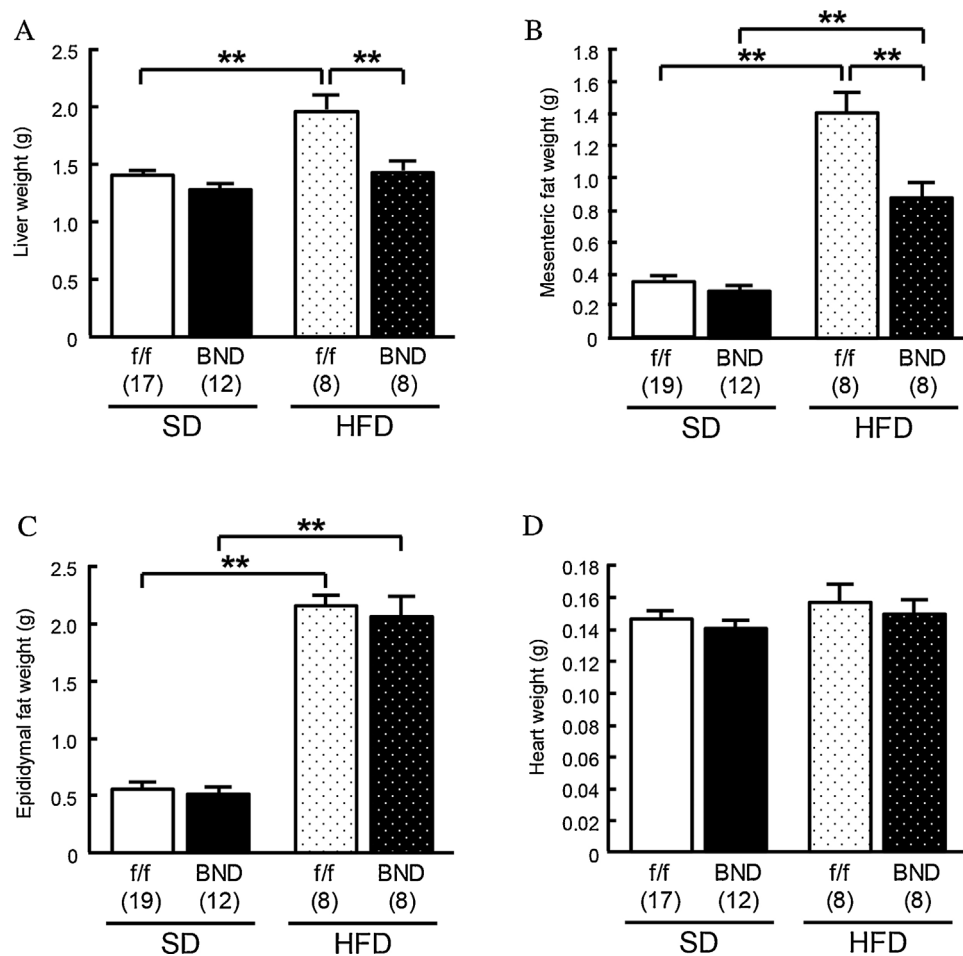
Fig. 4. Changes in tissue weight in BND mice. (A) Liver, (B) mesenteric fat, (C) epididymal fat, and (D) heart weight of mice at 16 weeks of age fed an SD or HFD. *$P < 0.05$, **$P < 0.01$. Values are means ± SEM. Number of animals is indicated in parentheses.

evaluate the mechanisms by which brain-specific NPR-B deletion prevented HFD-induced lipid accumulation in the mesenteric fat, we first determined the triglyceride content in white adipose tissue. In contrast to the liver, the triglyceride content in the white adipose tissue did not differ significantly between BND mice and control mice fed either an SD or HFD (S4 Fig.). Next, we analyzed the mRNA expression of genes involved in lipid metabolism and energy regulation in the white adipose tissue (Fig. 6A–U). Beige adipocytes, which sporadically reside within white adipose tissue, express UCP1 and exhibit UCP1-dependent thermogenic capacity [18]. Expression of UCP1 mRNA in the white adipose tissue was comparable between BND and control mice fed either an SD or HFD (Fig. 6P–R). In Western blot analysis of extracts from white adipose tissue, we did not detect UCP1 protein in control or BND mice fed either an SD or HFD (S5 Fig.). A marked change was observed in the mRNA expression of uncoupling protein 2 (UCP2), a critical regulator of cellular fuel utilization and whole body glucose and lipid metabolism [19]. The expression of UCP2 mRNA was significantly increased in the white adipose tissues in control mice fed an HFD (Fig. 6S–T). The UCP2 mRNA expression in the mesenteric fat of BND mice fed an HFD was significantly lower than in that of control mice (Fig. 6S). This difference was not observed in the epididymal fat or subcutaneous fat (Fig. 6T and U). As for skeletal muscle, the triglyceride content and UCP2 mRNA expression in the soleus did not differ significantly between BND and control mice (S6. Fig.).

3.8. Involvement of sympathetic nervous system in the effect of brain-specific NPR-B deletion on the liver and white adipose tissue

The brain controls metabolism in the liver and white adipose tissue via sympathetic innervation [20]. Norepinephrine is the main catecholaminergic transmitter and its content in a particular tissue reflects sympathetic nerve activity [21,22]. No significant difference in norepinephrine content in the liver and white adipose tissue (mesenteric fat and epididymal fat) between genotypes under either an SD or HFD (Fig. 7A–C).

3.9. Effect of short-term HFD feeding on hepatic and visceral lipid accumulation in BND mice

To investigate whether the protective effects of brain NPR-B deletion against HFD-induced hepatic and visceral lipid accumulation are independent of changes in body weight, we investigated the effects of short-term (1 week) HFD feeding on lipid metabolism in the liver and mesenteric fat. Without changes in body weight (S7 Fig. A), lipid accumulation in the liver and mesenteric fat in BND mice was comparable to that in control mice fed either an SD or HFD (S7 Fig. B and C). In addition, the expression levels of CD36 and Fsp27 mRNA in the liver and UCP2 mRNA in the mesenteric fat did not differ significantly between BND and control mice (S7 Figs. D–F).
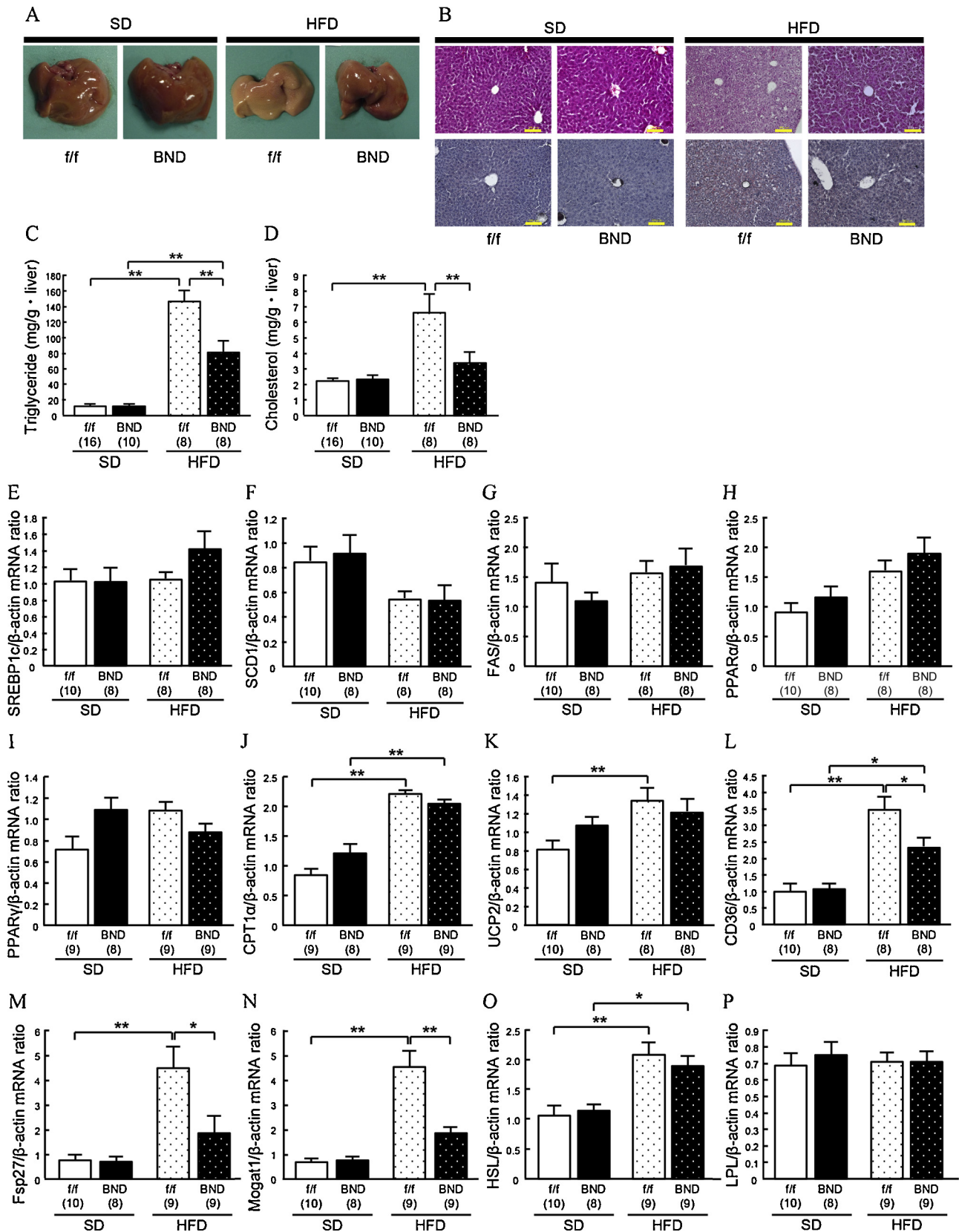
Fig. 5. Analysis of the liver in BND mice. (A) Representative images of mice at 16-weeks of age fed an SD or HFD. (B) Representative liver sections of mice at 16 weeks of age fed an SD or HFD (scale bar: 100 μm). Hematoxylin and eosin staining (upper panel). Oil red O staining (lower panel). (C) Liver triglyceride contents of mice at 16 weeks of age fed an SD or HFD. (D) Liver cholesterol contents of mice at 16s week of age fed an SD or HFD. (E)–(P) mRNA expression of genes involved in lipid metabolism in mice fed an SD or HFD at 16 week of age. Target gene mRNA expression levels were assessed by quantitative reverse transcription-PCR. Data were normalized to β-actin mRNA. *$P < 0.05$, **$P < 0.01$. Values are means ± SEM. Number of animals is indicated in parentheses.
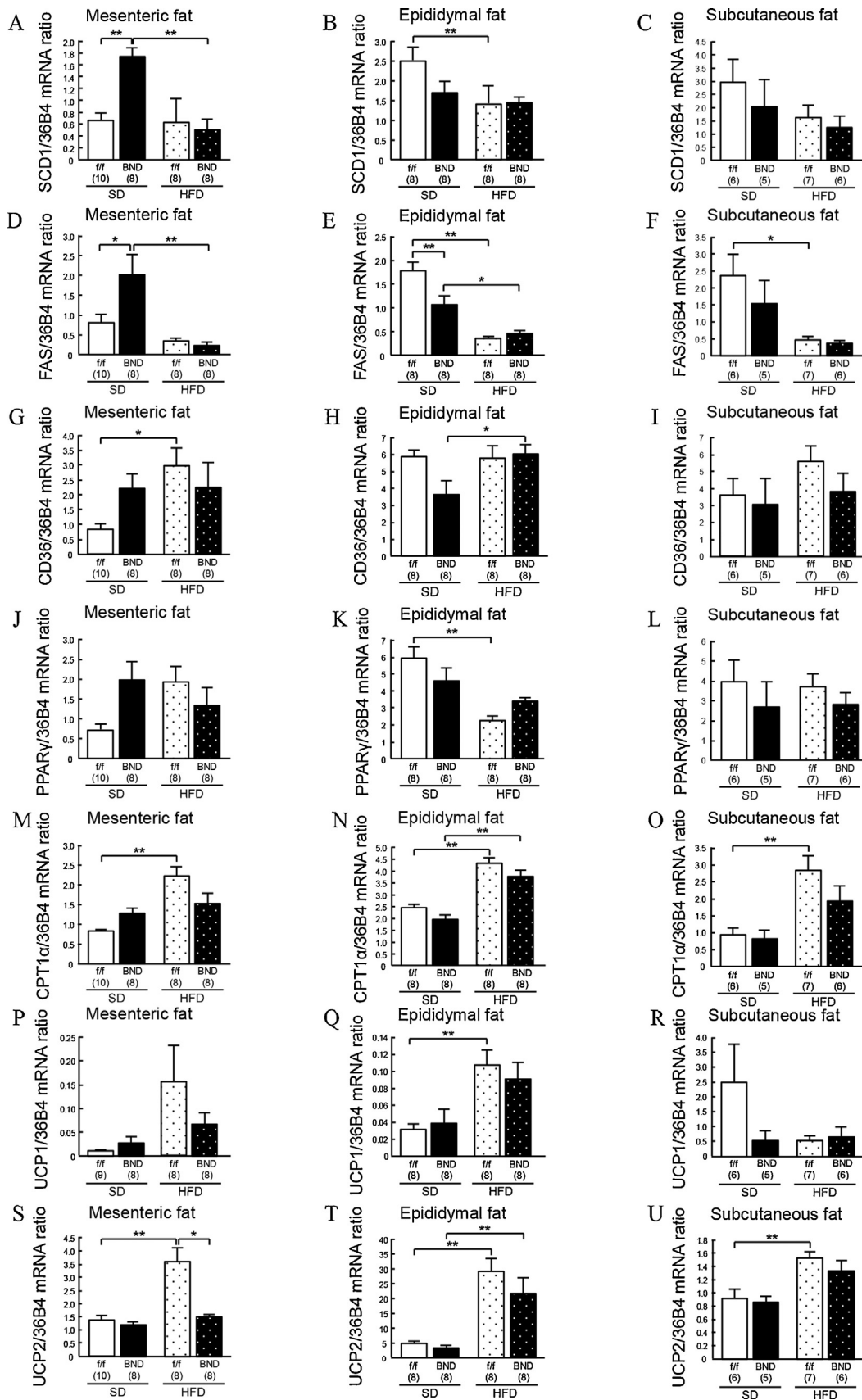
Fig. 6. mRNA expression of genes involved in lipid metabolism and energy regulation in white adipose tissue. mRNA expression of genes involved in lipid metabolism in mice fed an SD or HFD at 16 weeks of age in the mesenteric fat (A, D, G, J, M, P, S), epididymal fat (B, E, H, K, N, Q, T), and subcutaneous fat (C, F, I, L, O, R, U). Target gene mRNA expression levels were assessed by quantitative reverse transcription-PCR. Data were normalized to 36B4 mRNA.*$P<0.05$, **$P<0.01$. Values are means ± SEM. Number of animals is indicated in parentheses.
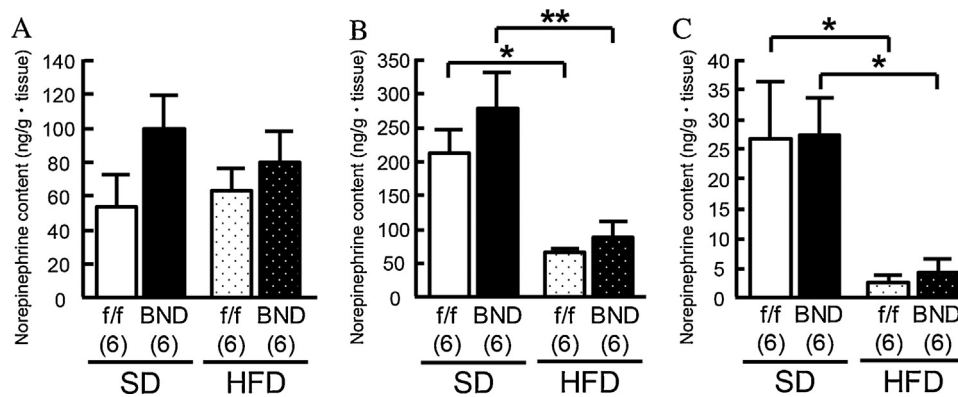
Fig. 7. Norepinephrine content in the liver and white adipose tissue in BND mice. Norepinephrine levels were measured in the (A) liver, (B) mesenteric fat, and (C) epididymal fat harvested from mice at 16 weeks of age. *$P < 0.05$, **$P < 0.01$. Values are means $\pm$ SEM. Number of animals is indicated in parentheses.

3.10. Changes in the hypothalamic peptide and cytokine mRNA expression levels in BND mice

Energy homeostasis and food intake are strictly controlled by regulatory centers in the hypothalamus. The brain and liver are connected both anatomically and functionally [23–26]. Therefore, we examined possible neural systems in the hypothalamus that might be involved in lipid accumulation in the mesenteric fat and liver.

We examined the mRNA expression of major orexigenic (neuropeptide Y [NPY] and Agouti-related peptide [AgRP]) and anorexigenic (pro-opiomelanocortin [POMC] and cocaine- and amphetamine-regulated transcript [CART]) neuropeptides, proinflammatory cytokines (TNFα, IL-1β, and IL-6), and peroxisome proliferator-activated receptors (PPARs; PPARα, PPARδ, and PPARγ) in the hypothalamus. As shown in Fig. 8 F, IL-1β mRNA expression was increased in BND mice fed an SD compared with control mice fed the same diet. Otherwise, there was no significant difference in the expression of these mRNAs between BND and control mice fed an SD or HFD (Fig. 8A–E, G–J).

4. Discussion

Obesity greatly increases the risk for several pathologies, including type 2 diabetes, cardiovascular disease, nonalcoholic fatty liver disease, and cancer [27–29]. High-energy intake, particularly the consumption of an HFD, promotes the development of obesity in humans and rodents. A characteristic of overweight or obese people is excessive lipid deposition in the visceral fat and liver, which leads to the progression of metabolic dysfunction including insulin resistance and dyslipidemia [30]. Recent studies revealed that the CNS, particularly the hypothalamus, is critical for regulating energy balance and nutrient metabolism [22–26].

The findings of the present study revealed that brain-specific NPR-B deletion prevented body weight gain and lipid accumulation in the liver and visceral fat associated with HFD feeding in mice. Hepatic triglyceride accumulation is controlled at several levels, including fatty acid uptake, synthesis and storage of triglycerides, fatty acid oxidation, and lipolysis [31]. The reduced HFD-induced fat deposition in the liver in BND mice was confirmed by histologic evaluation, and liver triglyceride and cholesterol contents. Gene expression analysis revealed significantly lower mRNA expression of CD36, Fsp27, and Mogat1 in the liver of BND mice fed an HFD compared with control mice. These findings indicate that fatty acid uptake, triglyceride storage, and synthesis in the liver were diminished in BND mice. On the other hand, expression of these genes is elevated in hepatic steatosis [32,33]. Moreover, there were no significant differences in the expression levels of CD36 and Fsp27 mRNA in the liver between BND and control mice under short-term

HFD feeding conditions. These findings suggest that the effects of brain NPR-B deletion on gene expression in the liver are secondary to changes in body weight.

Rodents have three morphologically distinct fat depots: subcutaneous, intra-abdominal, and visceral fat. Visceral fat, notably mesenteric fat, which is located in the area of the portal circulation, plays a critical role in the pathogenesis of metabolic syndrome [34–36]. The mesenteric fat weight was decreased in BND mice fed an HFD, while the epididymal fat weight was comparable to that in control mice. In addition, UCP2 mRNA expression in the mesenteric fat of BND mice fed an HFD was significantly lower than that of control mice. Interestingly, this difference was not observed in the epididymal fat or the subcutaneous fat. Recent data suggest that UCP2 functions as a metabolic switch that enables the promotion of fatty acid metabolism over glucose utilization [19]. Based on this hypothesis, under an HFD, brain-specific NPR-B deletion might lead to reduced mitochondrial fatty acid oxidation and increased glucose metabolism in the mesenteric fat. Under short-term HFD feeding conditions, however, there was no significant difference in UCP2 mRNA expression in the mesenteric fat between BND and control mice. This finding suggests that the decreased lipid deposition in the mesenteric fat in BND mice leads to reduced expression of UCP2 mRNA in the mesenteric fat.

We next examined how the information of altered brain CNP/NPR-B signaling is conveyed to the liver and mesenteric fat. Previous studies reported that CNP/NPR-B signaling inhibits SNS activity in rodents [14,37], therefore we focused on the importance of sympathetic innervation from the brain to the liver and visceral fat in energy metabolism. We measured the norepinephrine content in the liver and white adipose tissue as an index of SNS activity in these tissues. In the present study, however, we found no significant difference in the norepinephrine content in the liver and white adipose tissue. Moreover, there were no differences in body temperature, oxygen consumption, or UCP1 protein expression in the brown adipose tissue between BND and control mice. Together, these results suggest that SNS is unlikely to be the underlying mechanism.

The molecular targets of CNP/NPR-B signaling in the CNS are also unclear. The major brain region involved in the regulation of general energy balance is the hypothalamus. Within the arcuate nucleus of the hypothalamus, both NPY/AgRP expressing neurons and POMC expressing neurons influence lipid metabolism in various key target organs (i.e., liver, white adipose tissue, and brown adipose tissue). This process is at least in part mediated via the SNS [20]. Hypothalamic inflammation is also considered to be an important pathologic component in obesity and metabolic diseases [38]. In addition, recent evidence suggests that PPARs in the brain play a key role in lipid metabolism and inflammation in response
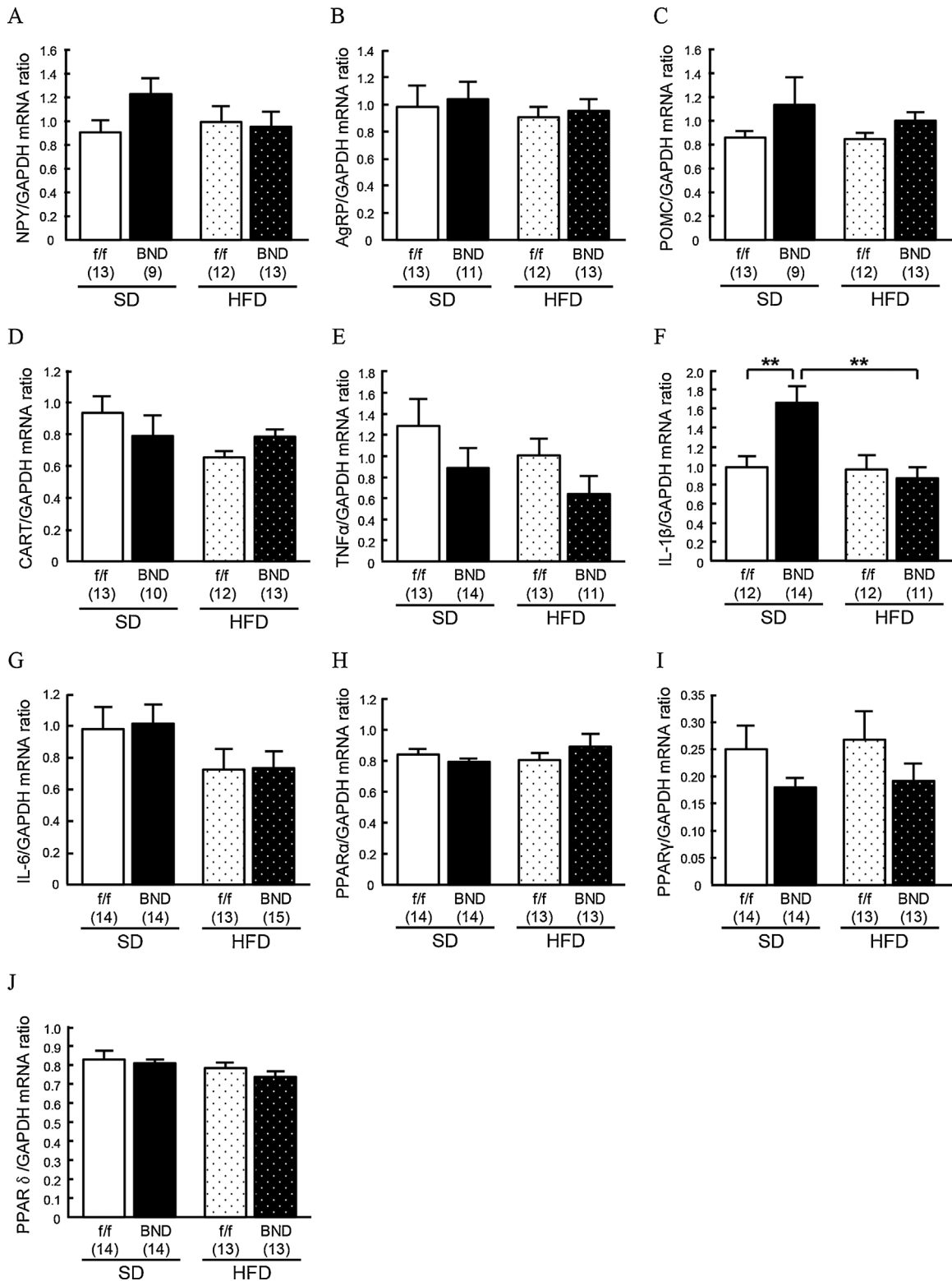
Fig. 8. mRNA expression in the hypothalamus in BND mice. Hypothalamic mRNA expression levels in BND and control mice fed an SD or HFD at 16 weeks of age. Target gene mRNA expression levels of (A) NPY, (B) AgRP, (C) pro-opiomelanocortin (POMC), (D) cocaine- and amphetamine-regulated transcript (CART), (E) TNFα, (F) IL-1β, (G) IL-6, (H) PPARα, (I) PPARγ, and (J) PPARδ were assessed by quantitative reverse transcription-PCR. Data were normalized to GAPDH mRNA. $*P < 0.05$, $**P < 0.01$. Values are means ± SEM. Number of animals is indicated in parentheses.

to dietary and endogenous fatty acid ligands [39–42]. Based on the present gene expression analysis, however, it is not likely that these factors make a major contribution to the effects of CNS CNP/NPR-B signaling on the liver and visceral fat.

We previously reported that CNP administered intracerebroventricularly significantly suppresses fasting-induced refeeding and nocturnal food intake in mice [15]. Therefore, we hypothesized that CNP/NPR-B signaling in the brain suppresses food intake. In the

present study, however, the amount of food intake did not differ significantly between BND mice and control mice fed either an SD or HFD. This discrepancy between pharmacologic and genetic studies is also reported for NPY and its receptors. Mice that lack the Y5 receptor, which is a possible mediator of the orexigenic response of NPY, develop mild late-onset obesity [43]. These discrepancies likely relate to the fact that there are redundant brain circuits that compensate for specific gene deficiencies.

A limitation of our study is that we examined the effects of brain-specific NPR-B deletion using Nestin-Cre mice. It has become increasingly recognized that Nestin-Cre mice have some background effects in terms of nonspecific gene deletion, as well as a metabolic phenotype [17]. First, in the Nestin-Cre line, expression of the Cre transgene is not specific to the brain, and is observed in several other tissues, such as the pancreas and kidneys [44,45]. Although we analyzed selective NPR-B deletion by quantitative RT-PCR, we cannot completely rule out the possibility that the phenotype observed in BND mice is due to nonspecific gene deletion. Second, Nestin-Cre mice that are commercially available from Jackson Laboratory exhibit a significantly reduced body length and weight when fed an SD compared with wild-type control mice [46]. This phenotype of Nestin-Cre mice is most likely a consequence of reduced growth hormone levels in these animals [47,48]. Our Nestin-Cre line was independently generated [16], and the gene construct of the mice differs from that of mice from the Nestin-Cre line from Jackson Laboratory. In addition, body weight did not differ among the wild-type, our Nestin-Cre, and floxed mice fed either an SD or HFD (S2 Fig. A and B). Moreover, neither plasma growth hormone and IGF-I levels, nor body length differed between BND and floxed mice (S2 Fig. C and D, and Fig. 1K). Therefore, we think our Nestin-Cre mice in the present study do not exhibit the metabolic changes observed in the Nestin-Cre mice obtained from Jackson Laboratory. To address these issues and to determine the precise role of the CNP/NPR-B system in energy homeostasis, further analysis using different strains of Cre-expressing mice, such as Synapsin-Cre, POMC-Cre, or AgRP-Cre mice, is required.

NPR-B mRNA is widely expressed throughout the nervous system, and abundantly expressed in the limbic cortex, neocortex, olfactory bulb, hypothalamus, hippocampus, amygdala, and the neural lobe of the pituitary [7]. *In situ* hybridization analysis revealed that the distribution of NPR-B in the brain has a largely neuronal phenotype [11]. NPR-B mRNA has been detected in astrocyte cultures, and CNP appears to be biologically active in these systems [49]. In our Nestin-Cre mice, the Nestin transgene does not appear to target all NPR-B expressing neurons and/or glial cells in the nervous system, as approximately 30% of NPR-B remains at the mRNA level after Nestin-Cre-mediated recombination. This may due to the low level of transgene expression, resulting in recombination in a selected population of neurons and/or glial cells. Incomplete deletion of NPR-B might also result from NPR-B expression in non-Nestin expressing cells, however, as it is reported that NPR-B mRNA is expressed in vascular smooth muscle cells [7]. In either case, functional NPR-B would remain in the brain, which might modulate the phenotypes observed in BND mice. In addition, immunohistochemical analysis showed NPR-B staining in the peripheral nerves [50,51]. Therefore, the described phenotypes might be, at least in part, due to deletion of NPR-B in the peripheral nervous system. In this case, further analysis using different strains of Cre-expressing mice would be effective to address these issues.

In conclusion, the present study provides novel and important insights regarding the importance of CNS CNP/NPR-B signaling in the regulation of visceral lipid metabolism and the development of hepatic steatosis, especially under HFD conditions. Further analyses of the precise mechanisms underlying the metabolic phenotype of BND mice and effects of CNP/NPR-B signaling in the brain will enhance our understanding of the significance of the CNP/NPR-B system in energy regulation.

Author contributions

Y.Y. researched the data and wrote the manuscript. N.Y-G. and G.K. contributed the study design and edited the manuscript. Y.O., Y.K., Y.M., K.K., N.K., M.M., A.Y., K.O., N.I., and K.N. contributed to the discussion and reviewed the manuscript. N.Y-G. is the guarantor of this work and, as such, had full access to all the data in the study and takes responsibility for the integrity of the data and the accuracy of the data analysis.

Appendix A. Supplementary data

Supplementary data associated with this article can be found, in the online version, at http://dx.doi.org/10.1016/j.peptides.2016.03.014.

References

[1] L.R. Potter, Natriuretic peptide metabolism, clearance and degradation, FEBS J. 278 (2011) 1808–1817.

[2] V. Leuranguer, P.M. Vanhoutte, T. Verbeuren, M. Félétou, C-type natriuretic peptide and endothelium-dependent hyperpolarization in the guinea-pig carotid artery, Br. J. Pharmacol. 153 (2008) 57–65.

[3] S. Del Ry, M. Cabiati, F. Vozzi, B. Battolla, C. Caselli, F. Forini, et al., Expression of C-type natriuretic peptide and its receptor NPR-B in cardiomyocytes, Peptides 32 (2011) 1713–1718.

[4] M. Suda, K. Tanaka, M. Fukushima, K. Natsui, A. Yasoda, Y. Komatsu, et al., C-type natriuretic peptide as an autocrine/paracrine regulator of osteoblast: evidence for possible presence of bone natriuretic peptide system, Biochem. Biophys. Res. Commun. 223 (1996) 1–6.

[5] K. Totsune, K. Takahashi, O. Murakami, K. Itoi, M. Sone, M. Ohneda, et al., Immunoreactive C-type natriuretic peptide in human adrenal glands and adrenal tumors, Peptides 15 (1994) 287–290.

[6] S.J. Nielsen, J.P. Gøtze, H.L. Jensen, J.F. Rehfeld, ProCNP and CNP are expressed primarily in male genital organs, Regul. Pept. 146 (2008) 204–212.

[7] L.R. Potter, S. Abbey-Hosch, D.M. Dickey, Natriuretic peptides, their receptors, and cyclic guanosine monophosphate-dependent signaling functions, Endocr. Rev. 27 (2006) 47–72.

[8] J.P. Herman, M.C. Langub, R.E. Watson, Localization of C-type natriuretic peptide mRNA in rat hypothalamus, Endocrinology 133 (1993) 1903–1906.

[9] M.C. Langub, R.E. Watson, J.P. Herman, Distribution of natriuretic peptide precursor mRNAs in the rat brain, J. Comp. Neurol. 356 (1995) 183–199.

[10] M.C. Langub, C.M. Dolgas, R.E. Watson, J.P. Herman, The C-type natriuretic peptide receptor is the predominant natriuretic peptide receptor mRNA expressed in rat hypothalamus, J. Neuroendocrinol. 7 (1995) 305–309.

[11] J.P. Herman, C.M. Dolgas, D. Rucker, M.C. Langub, Localization of natriuretic peptide-activated guanylate cyclase mRNAs in the rat brain, J. Comp. Neurol. 369 (1996) 165–187.

[12] H. Chusho, N. Tamura, Y. Ogawa, A. Yasoda, M. Suda, T. Miyazawa, et al., Dwarfism and early death in mice lacking C-type natriuretic peptide, Proc. Natl. Acad. Sci. U. S. A. 98 (2001) 4016–4021.

[13] N. Tamura, L.K. Doolittle, R.E. Hammer, J.M. Shelton, J.A. Richardson, D.L. Garbers, Critical roles of the guanylyl cyclase B receptor in endochondral ossification and development of female reproductive organs, Proc. Natl. Acad. Sci. U. S. A. 101 (2004) 17300–17305.

[14] M. Inuzuka, N. Tamura, N. Yamada, G. Katsuura, N. Oyamada, D. Taura, et al., C-type natriuretic peptide as a new regulator of food intake and energy expenditure, Endocrinology 151 (2010) 3633–3642.

[15] N. Yamada-Goto, G. Katsuura, K. Ebihara, M. Inuzuka, Y. Ochi, Y. Yamashita, et al., Intracerebroventricular administration of C-type natriuretic peptide suppresses food intake via activation of the melanocortin system in mice, Diabetes 62 (2013) 1500–1504.

[16] F. Isaka, M. Ishibashi, W. Taki, N. Hashimoto, S. Nakanishi, R. Kageyama, Ectopic expression of the bHLH gene Math1 disturbs neural development, Eur. J. Neurosci. 11 (1999) 2582–2588.

[17] E. Harno, E.C. Cottrell, A. White, Metabolic pitfalls of CNS cre-based technology, Cell Metab. 18 (2013) 21–28.

[18] L. Sidossis, S. Kajimura, Brown and beige fat in humans: thermogenic adipocytes that control energy and glucose homeostasis, J. Clin. Invest. 125 (2015) 478–486.

[19] S. Diano, T.L. Horvath, Mitochondrial uncoupling protein 2 (UCP2) in glucose and lipid metabolism, Trends Mol. Med. 18 (2012) 52–58.

[20] J.J. Geerling, M.R. Boon, S. Kooijman, E.T. Parlevliet, L.M. Havekes, J.A. Romijn, et al., Sympathetic nervous system control of triglyceride metabolism: novel concepts derived from recent studies, J. Lipid Res. 55 (2014) 180–189.

[21] I. Villanueva, M. Piñón, L. Quevedo-Corona, R. Martínez-Olivares, R. Racotta, Epinephrine and dopamine colocalization with norepinephrine in various peripheral tissues: guanethidine effects, Life Sci. 73 (2003) 1645–1653.

[22] J.P. Warne, F. Alemi, A.S. Reed, J.M. Varonin, H. Chan, M.L. Piper, et al., Impairment of central leptin-mediated PI3 K signaling manifested as hepatic steatosis independent of hyperphagia and obesity, Cell Metab. 14 (2011) 791–803.

[23] C.M. Knight, R. Gutierrez-Juarez, T.K. Lam, I. Arrieta-Cruz, L. Huang, G. Schwartz, et al., Mediobasal hypothalamic SIRT1 is essential for resveratrol's effects on insulin action in rats, Diabetes 60 (2011) 2691–2700.

[24] S. Purkayastha, H. Zhang, G. Zhang, Z. Ahmed, Y. Wang, D. Cai, Neural dysregulation of peripheral insulin action and blood pressure by brain endoplasmic reticulum stress, Proc. Natl. Acad. Sci. U. S. A. 108 (2011) 2939–2944.

[25] T.K. Lam, A. Pocai, R. Gutierrez-Juarez, S. Obici, J. Bryan, L. Aguilar-Bryan, et al., Hypothalamic sensing of circulating fatty acids is required for glucose homeostasis, Nat. Med. 11 (2005) 320–327.

[26] Q. Zhang, J. Yu, B. Liu, Z. Lv, T. Xia, F. Xiao, et al., Central activating transcription factor 4 (ATF4) regulates hepatic insulin resistance in mice via S6K1 signaling and the vagus nerve, Diabetes 62 (2013) 2230–2239.

[27] K.M. Flegal, B.I. Graubard, D.F. Williamson, M.H. Gail, Excess deaths associated with underweight, overweight, and obesity, JAMA 293 (2005) 1861–1867.

[28] G. Marchesini, E. Bugianesi, G. Forlani, F. Cerrelli, M. Lenzi, R. Manini, et al., Nonalcoholic fatty liver, steatohepatitis, and the metabolic syndrome, Hepatology 37 (2003) 917–923.

[29] K. Bhaskaran, I. Douglas, H. Forbes, I. dos-Santos-Silva, D.A. Leon, L. Smeeth, Body-mass index and risk of 22 specific cancers: a population-based cohort study of 5·24 million UK adults, Lancet 384 (2014) 755–765.

[30] J.P. Després, I. Lemieux, Abdominal obesity and metabolic syndrome, Nature 444 (2006) 881–887.

[31] J.K. Dowman, J.W. Tomlinson, P.N. Newsome, Pathogenesis of non-alcoholic fatty liver disease, QJM 103 (2010) 71–83.

[32] N. Guillén, M.A. Navarro, C. Arnal, E. Noone, J.M. Arbonés-Mainar, S. Acín, et al., Microarray analysis of hepatic gene expression identifies new genes involved in steatotic liver, Physiol. Genomics 37 (2009) 187–198.

[33] M. Radonjic, J.R. de Haan, M.J. van Erk, K.W. van Dijk, S.A. van den Berg, P.J. de Groot, et al., Genome-wide mRNA expression analysis of hepatic adaptation to high-fat diets reveals switch from an inflammatory to steatotic transcriptional program, PLoS One 4 (2009) e6646.

[34] B.L. Wajchenberg, Subcutaneous and visceral adipose tissue: their relation to the metabolic syndrome, Endocr. Rev. 21 (2000) 697–738.

[35] P. Björntorp, Portal adipose tissue as a generator of risk factors for cardiovascular disease and diabetes, Arteriosclerosis 10 (1990) 493–496.

[36] R.S. Ahima, J.S. Flier, Adipose tissue as an endocrine organ, Trends Endocrinol. Metab. 11 (2000) 327–332.

[37] T.H. Langenickel, J. Buttgereit, I. Pagel-Langenickel, M. Lindner, J. Monti, K. Beuerlein, et al., Cardiac hypertrophy in transgenic rats expressing a dominant-negative mutant of the natriuretic peptide receptor B, Proc. Natl. Acad. Sci. U. S. A. 103 (2006) 4735–4740.

[38] S. Purkayastha, D. Cai, Neuroinflammatory basis of metabolic syndrome, Mol Metab. 2 (2013) 356–363.

[39] M. Lu, D.A. Sarruf, S. Talukdar, S. Sharma, P. Li, G. Bandyopadhyay, et al., Brain PPAR-γ promotes obesity and is required for the insulin-sensitizing effect of thiazolidinediones, Nat. Med. 17 (2011) 618–622.

[40] K.K. Ryan, B. Li, B.E. Grayson, E.K. Matter, S.C. Woods, R.J. Seeley, A role for central nervous system PPAR-γ in the regulation of energy balance, Nat. Med. 17 (2011) 623–626.

[41] M.V. Chakravarthy, Y. Zhu, M. López, L. Yin, D.F. Wozniak, T. Coleman, et al., Brain fatty acid synthase activates PPARalpha to maintain energy homeostasis, J. Clin. Invest. 117 (2007) 2539–2552.

[42] H.E. Kocalis, M.K. Turney, R.L. Printz, G.N. Laryea, L.J. Muglia, S.S. Davies, et al., Neuron-specific deletion of peroxisome proliferator-activated receptor delta PPARδ in mice leads to increased susceptibility to diet-induced obesity, PLoS One 7 (2012) e42981.

[43] D.J. Marsh, G. Hollopeter, K.E. Kafer, R.D. Palmiter, Role of the Y5 neuropeptide Y receptor in feeding and obesity, Nat. Med. 4 (1998) 718–721.

[44] A. Delacour, V. Nepote, A. Trumpp, P.L. Herrera, Nestin expression in pancreatic exocrine cell lineages, Mech. Dev. 121 (2004) 3–14.

[45] N.C. Dubois, D. Hofmann, K. Kaloulis, J.M. Bishop, A. Trumpp, Nestin-Cre transgenic mouse line Nes-Cre1 mediates highly efficient Cre/loxP mediated recombination in the nervous system, kidney, and somite-derived tissues, Genesis 44 (2006) 355–360.

[46] N. Briancon, D.E. McNay, E. Maratos-Flier, J.S. Flier, Combined neural inactivation of suppressor of cytokine signaling-3 and protein-tyrosine phosphatase-1B reveals additive, synergistic, and factor-specific roles in the regulation of body energy balance, Diabetes 59 (2010) 3074–3084.

[47] C. Galichet, R. Lovell-Badge, K. Rizzoti, Nestin-Cre mice are affected by hypopituitarism, which is not due to significant activity of the transgene in the pituitary gland, PLoS One 5 (2010) e11443.

[48] J. Declercq, B. Brouwers, V.P. Pruniau, P. Stijnen, G. de Faudeur, K. Tuand, et al., Metabolic and behavioral phenotypes in Nestin-Cre mice are caused by hypothalamic expression of human growth hormone, PLoS One 10 (2015) e0135502.

[49] C.F. Deschepper, S. Picard, Effects of C-type natriuretic peptide on rat astrocytes: regional differences and characterization of receptors, J. Neurochem. 62 (1994) 1974–1982.

[50] I. Kishimoto, T. Tokudome, T. Horio, H. Chusho, K. Nakao, et al., C-type natriuretic peptide is a Schwann cell-derived factor for development and function of sensory neurones, J. Neuroendocrinol. 20 (2008) 1213–1223.

[51] C. Sogawa, H. Wakizaka, W. Aung, Z.H. Jin, A.B. Tsuji, T. Furukawa, et al., C-type natriuretic peptide specifically acts on the pylorus and large intestine in mouse gastrointestinal tract, Am. J. Pathol. 182 (2013) 172–179.